ARMY RESEARCH LABORATORY

Thermal Conductivity Measurement Setup for Low Temperature Characterization of Laser Materials

by Zachary D Fleischman and Tigran Sanamyan

ARL-TR-7120 September 2014

Army Research Laboratory
Adelphi, MD 20783-1138

ARL-TR-7120 **September 2014**

Thermal Conductivity Measurement Setup for Low Temperature Characterization of Laser Materials

Zachary D Fleischman and Tigran Sanamyan
Sensors and Electron Devices Directorate, ARL

REPORT DOCUMENTATION PAGE

Form Approved
OMB No. 0704-0188

1. REPORT DATE *(DD-MM-YYYY)*	**2. REPORT TYPE**	**3. DATES COVERED (From - To)**
September 2014	Final	March 2014–March 2015

4. TITLE AND SUBTITLE
Thermal Conductivity Measurement Setup for Low Temperature Characterization of Laser Materials

5a. CONTRACT NUMBER

5b. GRANT NUMBER

5c. PROGRAM ELEMENT NUMBER

6. AUTHOR(S)
Zachary D Fleischman and Tigran Sanamyan

5d. PROJECT NUMBER
Frontier

5e. TASK NUMBER

5f. WORK UNIT NUMBER

7. PERFORMING ORGANIZATION NAME(S) AND ADDRESS(ES)
U.S. Army Research Laboratory
ATTN: RDRL-SEE-L
2800 Powder Mill Road
Adelphi, MD 20783-1138

8. PERFORMING ORGANIZATION REPORT NUMBER
ARL-TR-7120

9. SPONSORING/MONITORING AGENCY NAME(S) AND ADDRESS(ES)

10. SPONSOR/MONITOR'S ACRONYM(S)

11. SPONSOR/MONITOR'S REPORT NUMBER(S)

12. DISTRIBUTION/AVAILABILITY STATEMENT
Approved for public release; distribution unlimited.

13. SUPPLEMENTARY NOTES

14. ABSTRACT
We have developed a setup for accurately measuring the thermal conductivity κ of solid dielectric samples in the temperature range of 20–350 K. This setup makes use of a cryogenic refrigerator and several custom fixtures that together allow for fine temperature control and low thermal losses across the sample. Initial benchmark κ measurements of an undoped single-crystal yttrium aluminum garnet (YAG) sample show good agreement with literature from cryogenic to room temperature. We present thermal conductivity results for a series of ceramic yttria samples with varying erbium (Er) concentration. These results show the expected trend of decreased thermal conductivity with increased dopant content.

15. SUBJECT
Thermal conductivity, cryogenic, laser, oxide, ceramic

16. SECURITY CLASSIFICATION OF:			**17. LIMITATION OF ABSTRACT**	**18. NUMBER OF PAGES**	**19a. NAME OF RESPONSIBLE PERSON**
a. REPORT	**b. ABSTRACT**	**c. THIS PAGE**			Tigran Sanamyan
Unclassified	Unclassified	Unclassified	UU	22	**19b. TELEPHONE NUMBER** *(Include area code)* 301-394-2044

Standard Form 298 (Rev. 8/98)
Prescribed by ANSI Std. Z39.18

Contents

List of Figures

Acknowledgments

We gratefully acknowledge the financial support from the Frontier research fund of the US Army Research Laboratory's (ARL) Sensors and Electron Devices Directorate.

INTENTIONALLY LEFT BLANK.

1. Introduction

The first idea of operating lasers at cryogenic temperatures dates back to the early 1960s, immediately following the invention of solid-state lasers. However, this concept gained maturity only in the mid-90s due mostly to the progress in transparent, laser-grade ceramics and semiconductor pump sources. The main limiting factors for power scaling of room temperature solid-state lasers are thermal effects, such as thermal lensing, induced polarization losses, and fracture.

These detrimental thermal effects can be substantially suppressed by cryogenic cooling. The thermal conductivity of the gain medium is strongly increased, mainly due to the increase of the mean free path length of phonons, resulting in the decrease of temperature gradients. As an example, the thermal conductivity of yttrium aluminum garnet (YAG) increases by a factor of 7 when the temperature is reduced from 300 K to 77 K.[1] The thermal expansion coefficient and the thermooptic coefficient (dn / dT) are also reduced. All aforementioned thermal modifications at low temperature eventually affect the thermal lensing from bulging and stress.

The cryogenic temperatures also modify the spectroscopic characteristics of the laser media. The emission and absorption cross sections of dopant ions are increased, due to narrowing of spectral lines at low temperature. The thermal population of the lower laser level in quasi-three-level gain media is reduced, which again reduces the threshold pump power and leads to laser designs with increased power, efficiency, beam quality, etc. Therefore, cryogenic lasers open new opportunity for extending the operating wavelengths and substantially increase the efficiency and power of existing room temperature lasers.

A possible concern is that the bandwidth of both the emission and absorption of the cryogenic laser host may be reduced down to less than 1 nm, introducing more stringent requirements on linewidth and emission peak stability of pumps. Fortunately, the recent progress in semiconductor pump sources, such as development by industry of high power spectrally narrowed diode lasers, allow for the building of kW level cryogenic solid-state lasers.[2]

Although the cryogenic concept is mostly applicable to so-called low quantum defect lasers, where the heat deposition is kept at the very minimum, using this approach we recently demonstrated a diode-pumped, cryogenically cooled 2.7-µm erbium (Er^{3+}):yttria (Y_2O_3) ceramic laser, operating on quasi-three-level transitions. We demonstrated 14 W of continuous wave (CW) optical power and nearly diffraction-limited output; and this output was strictly pump power-limited.[3] Nearly quantum defect (QD)-limited 27.5% optical-to-optical slope efficiency[3] was largely achieved due to implementation of sufficiently narrowband high power pump source, a surface-emitting distributed feedback (SE-DFB) laser.

All of the above justifies the necessity of accurate thermal characterization of laser host materials at a wide temperature range from liquid helium to room temperatures. Among the thermal properties of materials, perhaps, the thermal conductivity is the most informative from a laser simulation and modeling perspective, and performance prediction as well.

This research is even more important for ceramic laser materials, where the thermal properties are strongly affected by the quality of material fabrication.

2. Theory and Experimental Setup

Thermal conductivity (κ) is the physical property of a material gauging how well it can transfer heat. In general, materials with high thermal conductivity are widely used in heat sink applications while materials with low thermal conductivity are commonly used as thermal insulators.

On the microscopic scale, heat transport in amorphous and crystalline dielectric solids is carried out through elastic vibrations of the crystal lattice, also known as phonons. In general, a longer phonon mean-free-path leads to much more effective heat transfer and a higher thermal conductivity. This phonon-dependence is one of several factors leading to the strong influence of temperature on thermal conductivity. Figure 1 shows the typical temperature dependence of thermal conductivity for dielectric solids, characterized by a peak separating two regions of steep decline. The temperature dependence of κ in Region 1 is largely defined by changes in the mean-free-path of the phonons in the material. At high temperatures, the basic mechanism limiting mean-free-path is scattering among phonons. Since scattering frequency depends on the overall number of phonons, and this number is proportional to temperature (T), it follows that $\kappa \propto T^{-1}$ in Region 1. At low temperatures (Region 2), the mean-free-path increases to such an extent that it becomes comparable to, and eventually even limited by, the width of the test sample. In this limiting case and for all lower temperatures, the mean-free-path is now a constant determined by the dimensions of the sample. Thus, in this temperature region, the only temperature-dependent quantity that has bearing on κ is the heat capacity C, which varies proportionally to T^3 at low temperatures. This leads to the steep decline in κ as sample temperature approaches zero.[4]

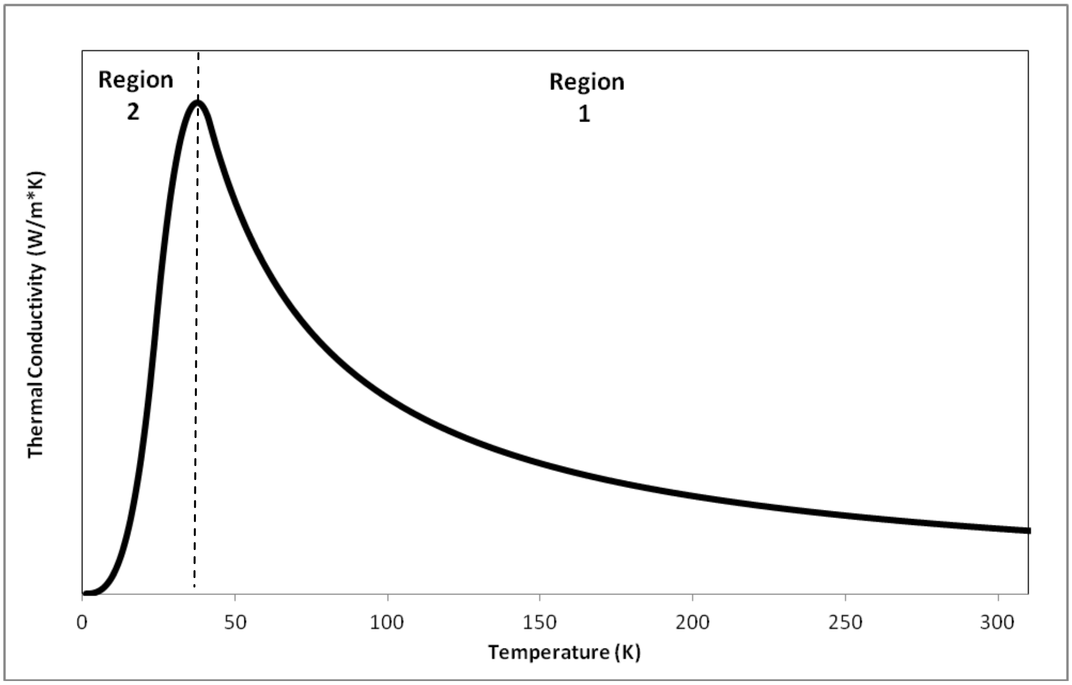

Fig. 1 Thermal conductivity as a function of temperature for typical dielectrics

Temperature is not the only factor that can influence thermal conductivity; the purity of the dielectric solid also plays a significant role. Chemical impurities, grain boundaries, and lattice imperfections can greatly reduce κ by providing additional scattering pathways that limit the mean-free-path of heat-transferring phonons. Considerations of sample purity are especially important in dielectrics designed to be laser gain media, which often have fluorescing impurities purposely doped into them. In such materials, the careful balance of dopant concentration and suitable thermal properties is crucial for optimal laser performance.

In practice, the determination of thermal conductivity always involves the measurement of the heat flux through the sample and the temperature gradient between opposite surfaces of the sample. Heat flux is defined as the amount of heat (Q) passing through a given cross section (A), while the temperature gradient is simply the change in temperature (ΔT) over a given length (L). Thermal conductivity (κ) is thus defined as

$$\kappa = \frac{\text{heat flux}}{\text{thermal gradient}} = \frac{Q/A}{\Delta T/L} = \frac{QL}{A\Delta T} \tag{1}$$

and is typically presented in the units $W/m \cdot K$. For a sample of known dimensions, the difficulty of the thermal conductivity measurement is in accurate determination of ΔT and Q. In experiments where Q is known (for example, when supplying a known power to a heating element), the measurement of κ is deemed absolute. Alternatively, if Q is known indirectly (by comparison), the method is called comparative. Whatever the method, the most accurate results

will come when the entire heat flux is uniaxial, meaning that is has to flow through the sample. For this reason, the heat losses or gains must be minimized in the radial direction.

Figure 2 shows the overall schematic of our thermal conductivity measuring setup, which was designed around two copper plate fixtures that can be attached to the superstructure of a CTI Cryodyne cryogenic refrigerator. The upper copper plate attaches directly to the cryofridge assembly, while the lower plate connects via four 6-32 nylon screws attached from the bottom. The sample to be measured gets sandwiched between the two copper plates, with thin indium layers (~0.2 mm thick) ensuring good thermal contact between the sample and the copper. Accurate temperature readings are obtained using DT-670-SD silicon diode sensors (Lakeshore), which have been indium-soldered to the upper and lower copper plates near the sample contact area. These sensors are read using a Lakeshore Model 224 temperature monitor. The lower copper plate has a thick-film chip resistor (State of the Art, Inc) soldered to the bottom, which can generate up to 100 W of heating power. We use a Keithley 2200-60-2 programmable power supply as the electrical source for this lower heater. Not shown in Fig. 2 is an aluminum intermediate heat shield that attaches to the upper copper plate and enshrouds the entire setup. This shield is necessary to mitigate any radiative heat transfers that might occur between the sample and the dewar tail of the cryofridge.

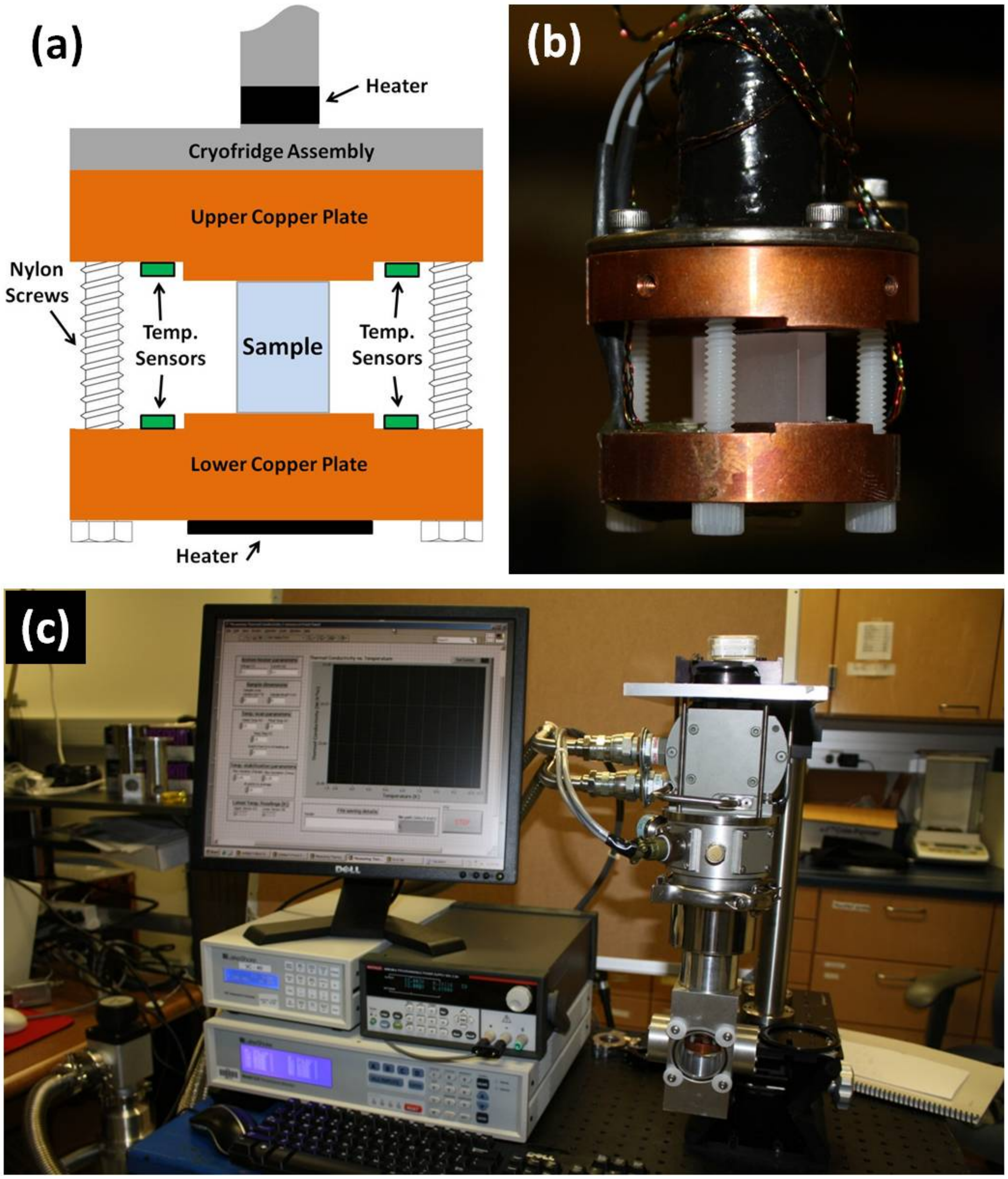

Fig. 2 a) A schematic of the thermal conductivity measuring setup attached to the cryofridge assembly. Wires have been omitted for clarity. b) A picture of the finished setup fixtures with a sample in place. c) The entire thermal conductivity measuring station.

Interfacing with the cryogenic refrigerator offers several benefits. The first of which is that we can make use of the built-in vacuum capabilities to greatly reduce radial heat losses/gains for greater accuracy in κ measurements. Additionally, the instrument is capable of fine temperature control between 10 and 350 K using the onboard cooling and attached heater (as well as a Lakeshore Model 325 temperature controller), allowing us to measure κ at any temperature in that range. This temperature control is also useful in that it allows the cryofridge to act as a

thermal sink, essentially keeping the upper copper plate and that side of the test sample at a constant set temperature no matter how much heat is applied to the lower copper plate.

Our method for measuring thermal conductivity invokes the steady-state approach, meaning that a κ value is not acquired until the temperature at each point of the sample is constant. Figure 3 shows the LabVIEW front panel for our thermal conductivity measuring program, which includes an example data set further illustrating the flow of an experiment. First, the cryofridge is driven to the temperature at which the measurement will be made using an independent controller, and the temperature sensor readings above and below the sample are allowed to reach steady-state. Then, a power value is selected for the lower heater in order to achieve a small (5–6 K) temperature gradient across the sample. The sample dimensions (L and A) are then input into the LabVIEW program in order to properly calculate κ. The final preparatory step is choosing a frequency for subsequent data points to be displayed; typically set to 2 s. When the program is finally initialized, the set power is applied to the lower heater and various parameters (time, upper and lower temperatures, and κ) are recorded and displayed at the chosen frequency. As the experiment progresses, the lower plate increases in temperature until steady-state is achieved; the upper plate is held at a constant temperature throughout the course of the experiment. The graphical display on the program front panel shows the progress as the calculated κ value converges to a constant.

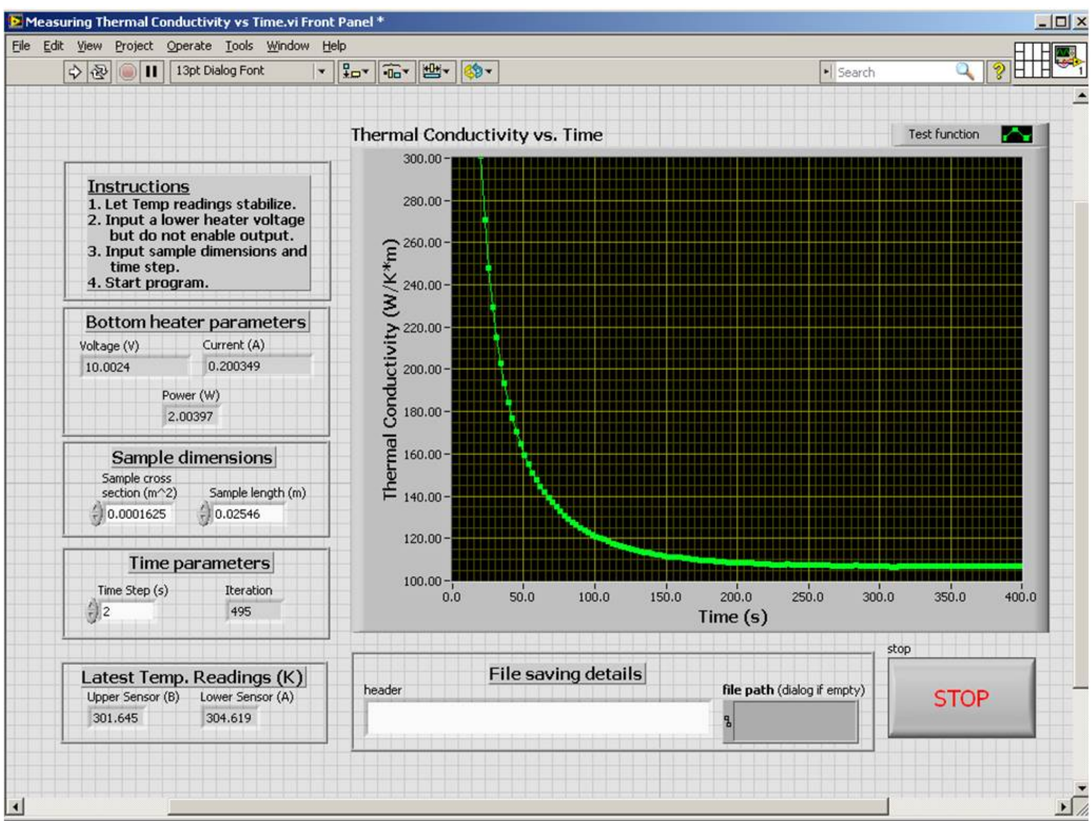

Fig. 3 Front panel of the thermal conductivity measurement LabVIEW program showing a sample data acquisition

While the setup and overall experiment were designed to achieve the highest possible accuracy in thermal conductivity measurements, several important issues had to be considered before κ values could be recorded effectively. The first issue was to get a feel for the baseline thermal transport in the non-sample connections between the two copper plates. This would include the nylon screws and the wires connecting the lower temperature sensors and heater. These components were chosen to minimize any leakage heat (nylon has κ ~0.25 W/m*K and the wires are small diameter), but their heat transport might be comparable to samples with low κ values. A series of measurements was performed at various temperatures with no sample in the setup; a power of 0.045 W was supplied to the lower heater at each test temperature and the steady-state thermal gradient between the two copper plates was measured. With these results, we were able to determine the thermal resistivity ($\Delta T/Q$) of the non-sample connections as a function of temperature, which is presented in Fig. 4. As can be seen, the results indicate that thermal leakage should be fairly minimal; nevertheless, this leakage value can easily be subtracted out of actual sample measurements, thereby improving their overall accuracy.

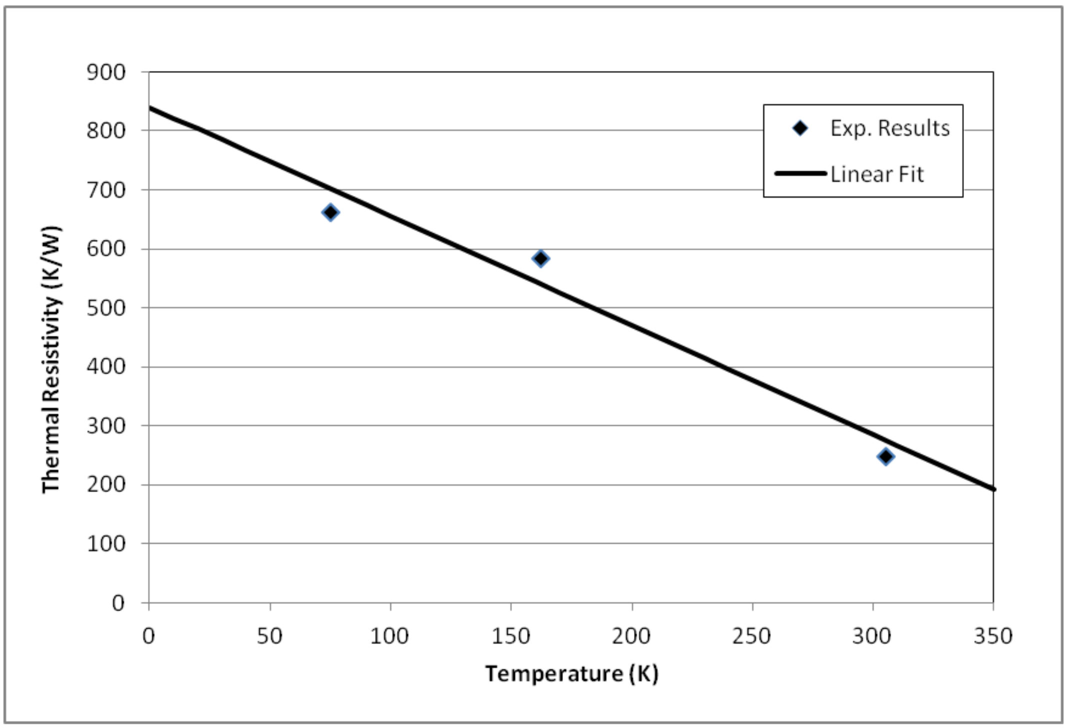

Fig. 4 Baseline thermal resistivity of all non-sample connections between the upper and lower copper plates. A power of 0.045 W was supplied to the lower heater.

Another important issue that must be considered whenever a new material is measured is the orientation of the sample in the experimental setup. In general, when the thermal conductivity is high, it is beneficial for the sample to be oriented such that L is large and A is small. This is because heat flux will be fairly high and a larger sample length and smaller area will establish a reasonably high thermal gradient, which can be accurately measured. Conversely, if κ is low, a shorter length and larger area are required to achieve sufficient thermal gradient. Additionally,

with low κ will also come low heat flux, meaning that lateral heat losses are much more of an issue. Thus, the smaller lateral surface area of samples in this orientation will help to mitigate these losses.

3. Preliminary Thermal Conductivity Measurements

As a first test of our thermal conductivity setup, we chose to measure κ for one of the most well-documented laser gain materials: undoped single-crystal YAG ($Y_3Al_5O_{12}$). We obtained a test sample of dimension 10x10x5 mm from Scientific Materials Corp. Because the κ for YAG is known to be fairly high, we oriented the sample such that the length L=10 mm and the cross-sectional area A=50 mm^2.

Figure 5 shows our results for κ as a function of temperature between 50 and 300 K, as well as results from two references, 5 and 6. It can be seen that there is fairly good agreement between the various experiments. In fact, there is no more than 10% deviation from a best fit line among all of the displayed values. Unfortunately, in our experiments, no values of κ could be reliably obtained below 50 K because the heat flux through our test sample was too high to obtain a decent thermal gradient. A sample with longer length or smaller cross sectional area should correct this problem and allow us to see the peak-like nature of κ at extremely low temperature.

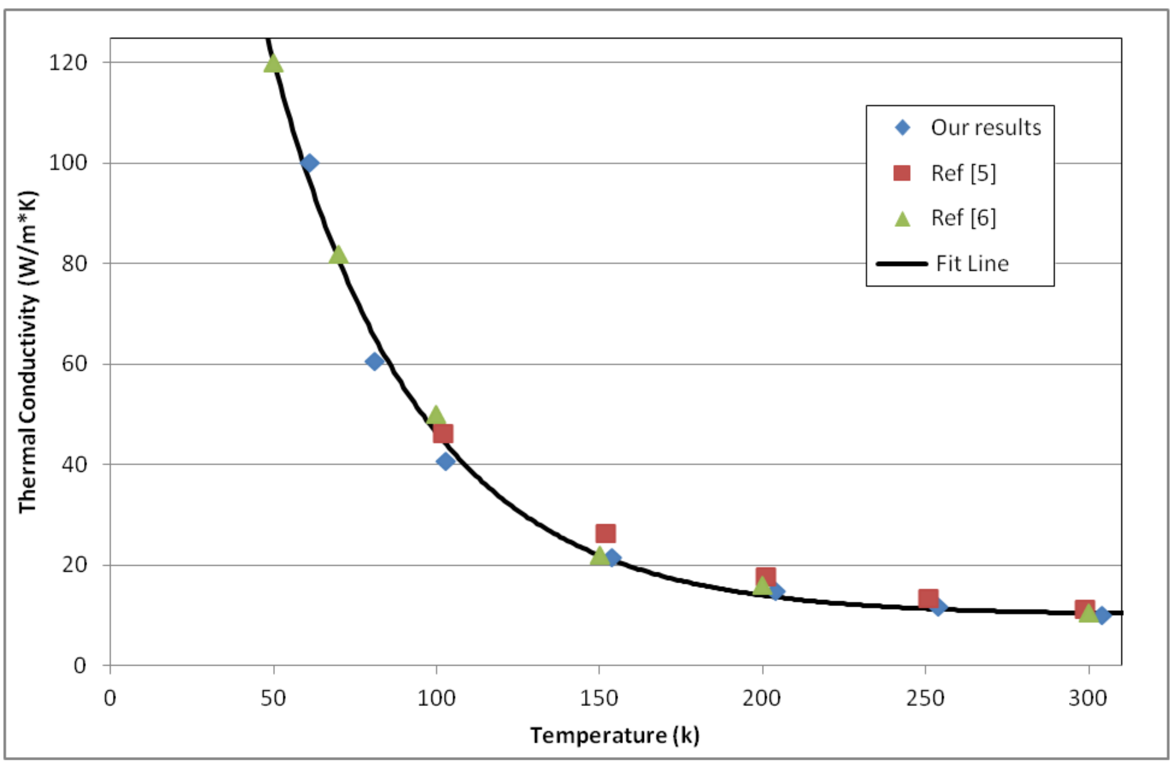

Fig. 5 Our experimental results for thermal conductivity of undoped single-crystal YAG as well as the results from two references, 5 and 6

With a successful benchmark test completed, we moved on to thermal conductivity measurements of materials that are of current interest in our laser-based research efforts. This entailed measuring a series of ceramic Y_2O_3 samples with varying Er content, obtained from Konoshima Chemical Co, Ltd. All samples were approximately 30x10x4 mm and were oriented in the setup such that the length L=10 mm and the cross-sectional area A=120 mm^2.

Figure 6 shows the results of our thermal conductivity measurements for Er-doped ceramic Y_2O_3 over the temperature range 20–300 K. We were able to extend our measured temperature range lower in these measurements because of the overall reduced thermal conductivity (lower heat flux) intrinsic to these samples compared to YAG. Thus, we are able to see the κ peak at low temperature. Immediately apparent in the results for this series of samples is the trend that increasing the doping content leads to lower thermal conductivity. This phenomenon is attributed to an increase in phonon-scattering, which inherently follows from decreasing purity in the higher-doped samples. While there are no direct comparisons in literature for this series of samples, our values are comparable to similar rare-earth doped ceramics.[7]

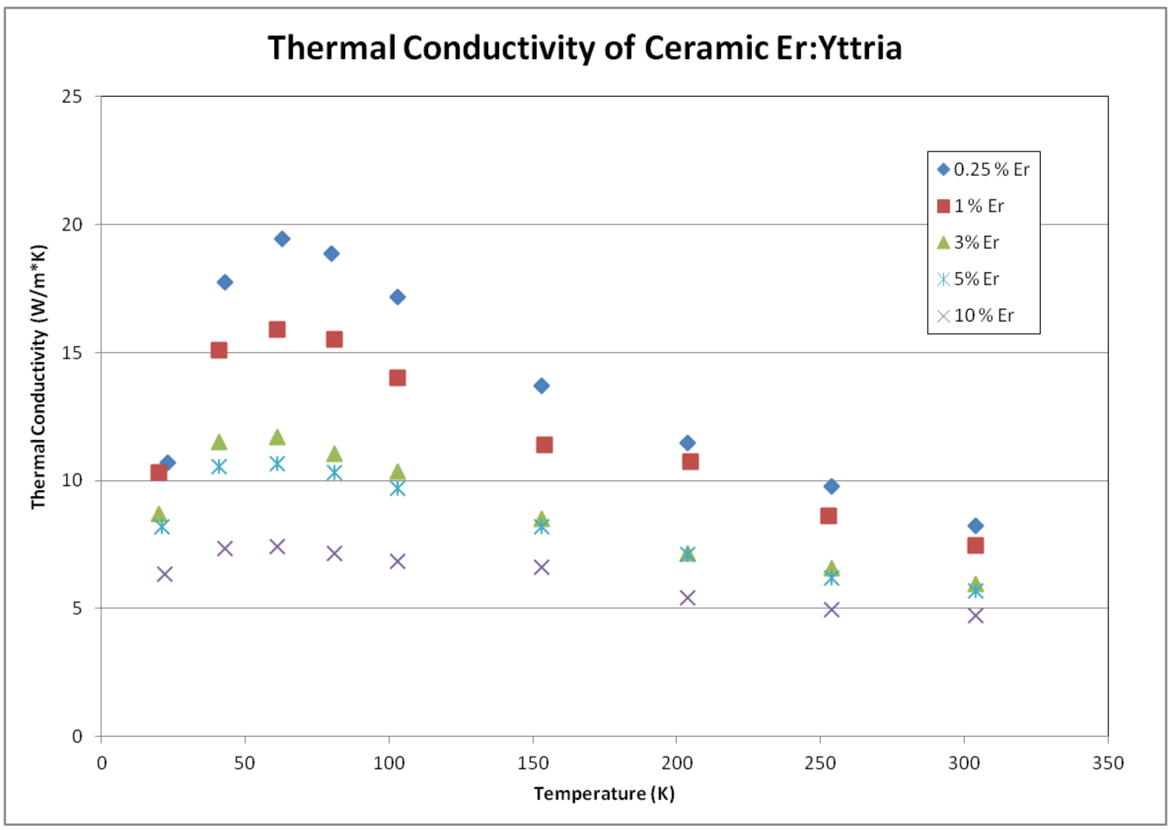

Fig. 6 Thermal conductivity results for ceramic yttria doped with varying amounts of Er

4. Conclusions

Our work with laser-gain media necessitates our accurate knowledge of the materials' thermal properties. Toward this end, we have designed and built a custom thermal conductivity measuring setup. Preliminary measurements of κ with respect to temperature for undoped single-crystal YAG have shown that our results are in good agreement with similar results obtained in other groups and with other measuring techniques. With our setup thoroughly vetted, we proceeded to measure the thermal conductivity for materials of interest in our laser research, namely, a series of ceramic Y_2O_3 samples with varying degrees of Er dopant.

5. References

1. Fa TY, Ripin DJ, Aggarwal RL, Ochoa JR, Chann B, Tilleman M, Spitzberg J. IEEE J. Sel. Topics Quantum Electron. 2007;13:448.
2. Brown DC, Singley JM, Kowalewski K, Guelzow J, Vitali V. Opt. Express. 2010;18:24770.
3. Sanamyan T, Kanskar M, Xiao Y, Kedlaya D, Dubinskii, M. Opt. Express. 2010;19:A1082.
4. Kittel Charles. Introduction to Solid State Physics, 7th Ed., Wiley, 1996.
5. Aggarwal RL, Ripin DJ, Ochoa JR, Fan TY. J. Appl. Phys. 2005;98:103514.
6. Slack GA, Oliver DW. Phys Re. B. 1971;4:592.
7. Sanghera J, Kim W, Villalobos G, Shaw B, Baker C, Frantz J, Sadowski B, Aggarwal I. Materials. 2012;5:258.

List of Symbols, Abbreviations, and Acronyms

A	cross-sectional area
ARL	US Army Research Laboratory
C	heat capacity
CW	continuous wave
dn/dT	thermooptic coefficient
Er	erbium
κ	thermal conductivity
L	sample length
Q	heat
QD	quantum defect
SE-DFB	surface emitting distributed feedback
T	temperature
ΔT	change in temperature
Y_2O_3	yttria
YAG	yttrium aluminum garnet

1 (PDF)	DEFENSE TECH INFO CTR ATTN DTIC OCA
2 (PDF)	US ARMY RSRCH LABORATORY ATTN IMAL HRA MAIL & RECORDS MGMT ATTN RDRL CIO LL TECHL LIB
1 (PDF)	GOVT PRNTG OFC ATTN A MALHOTRA
8 (PDF)	US ARMY RSRCH LAB ATTN RDRL SEE L Z D FLEISCHMAN T SANAMYAN G NEWBURGH J ZHANG L MERKLE M DUBINSKIY N TER-GABRIELYAN V FROMZEL

INTENTIONALLY LEFT BLANK.